

Semiclassical simulations of peripheral heavy-ion collisions at Fermi Energies and the sensitivity to the density dependence of the nuclear symmetry energy

G. A. Souliotis, D. V. Shetty, S. Galanopoulos, and S. J. Yennello

During the last several years we have undertaken a systematic study of heavy residues formed in quasi-elastic and deep-inelastic collisions near and below the Fermi energy. The original motivation of these studies was the understanding and the optimization of the production of very neutron-rich rare isotopes in these collisions [1,2,3]. In parallel, we became motivated to pursue these studies further in hopes of extracting information on the properties of the nuclear effective interaction as manifested in the mechanism of nucleon exchange and the course towards N/Z equilibration [4].

Recently, we focussed our interest on the possibility of extracting information on the isospin part of the nuclear equation of state (EOS) by comparing

our heavy residue data to detailed calculations using microscopic models of heavy-ion collisions at these energies [5]. After some initial efforts with transport-type codes (BUU, BNV), we turned our attention to the quantum molecular dynamics approach (QMD). We have performed detailed calculations using the recent version of the constrained molecular dynamics code CoMD of A. Bonasera and M. Papa [6,7]. This code is especially designed for reactions near and below the Fermi energy. It

implements an effective interaction corresponding to a nuclear-matter compressibility of $K=200$ (soft EOS) with several forms of the density dependence of the nucleon-nucleon symmetry potential (Fig. 1) [8]. While not using antisymmetrized N-body wave functions, CoMD imposes a constraint in the phase space occupation for each nucleon, effectively restoring the Pauli principle at each time step of the

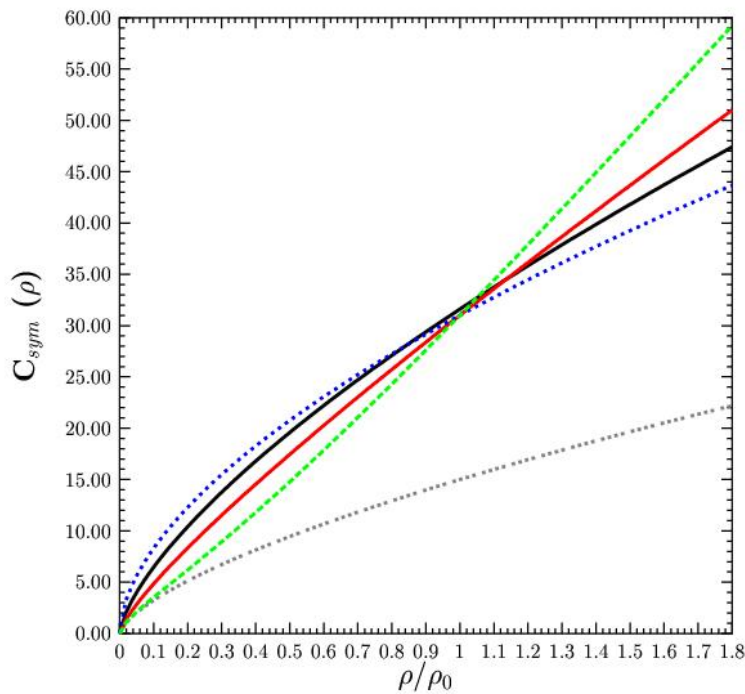


Figure 1. Density dependence of the nuclear symmetry energy $C_{sym}(\rho)$ corresponding to the choices of the nucleon-nucleon symmetry potential in the CoMD code: blue (asy-soft), red: (asy-stiff), green (super asy-stiff) and grey line (no-symm). The black line represents the form $31.6(\rho/\rho_0)^{0.69}$ consistent with the isoscaling analysis of IMFs from central heavy-ion collisions [8].

collision. This constraint preserves the fermionic nature of the interacting nuclei in a satisfactory manner [6]. The latest version (CoMD-II) also fully preserves the total angular momentum along with linear momentum and energy [7].

Results of the calculations and comparisons with our residue data are shown in Figs. 2-5. Fig. 2 shows the calculated average quasiprojectile angle (upper panel) and excitation energy per nucleon (lower panel) as a function of the mass of the (primary) quasiprojectiles. The black line corresponds to the prediction of the deep-inelastic transfer (DIT) code of Tassan-Got that has been extensively used in our studies of quasiprojectile formation near the Fermi energy [9]. The light blue curve shows the prediction of the heavy-ion phase-space exploration (HIPSE) model [10]. The remaining four lines are the results of CoMD calculations with symmetry potential options referred to as: “asy-soft” (blue line), “asy-stiff” (red line), “super asy-stiff” (green line) and “no-symm” (grey line). The first three forms correspond to a dependence of the symmetry-potential V_{symm} on the $\frac{1}{2}$, 1 and 2 power of the density, respectively, whereas in the last case (“no-symm”) this potential is set to zero - thus, only the kinetic part of the symmetry energy plays a role in this case (see, also Fig. 1). The CoMD calculation was stopped at $t=300$ fm/c. We observe differences between the predictions of DIT, HIPSE and CoMD that we will try to further investigate and understand in the near future. Regarding CoMD, despite the observed fluctuations of the mean values, we may tentatively conclude that the mean quasiprojectile angle is not sensitive to the choice of the symmetry potential. However, the mean excitation energy shows some sensitivity in the choice that deserves further exploration.

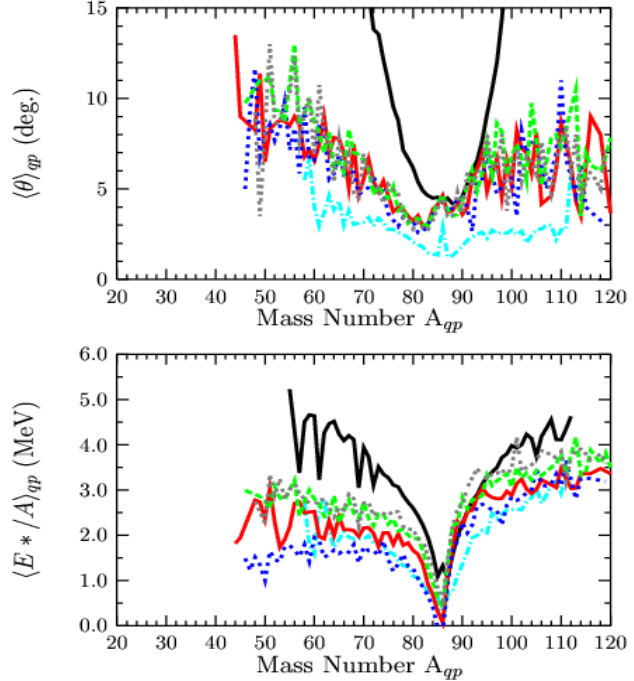


Figure 2. Mean quasiprojectile angle (upper panel) and excitation energy per nucleon (lower panel) as a function of quasiprojectile mass for the reaction $^{86}\text{Kr}(25\text{MeV/nucleon}) + ^{124}\text{Sn}$. Black line: DIT. Light-blue line: HIPSE. Blue (asy-soft), red (asy-stiff), green (super asy-stiff) and grey (no-symm).

In Fig. 3, the distributions of the mean angle, mean velocity and yield as a function of the mass of the (final) observable fragments are shown. The deexcitation of the primary fragments was done with the sequential decay code GEMINI [11]. The meaning of the curves is as before: black line: DIT, coloured lines: CoMD. The top panel shows, along with the calculations, the angular acceptance of the MARS separator $\Delta\theta=3^\circ\text{-}6^\circ$ for our measurements (dashed horizontal lines). In the middle and lower panels, the MARS data [1] are shown with solid symbols. The calculations in both cases are filtered with the angular

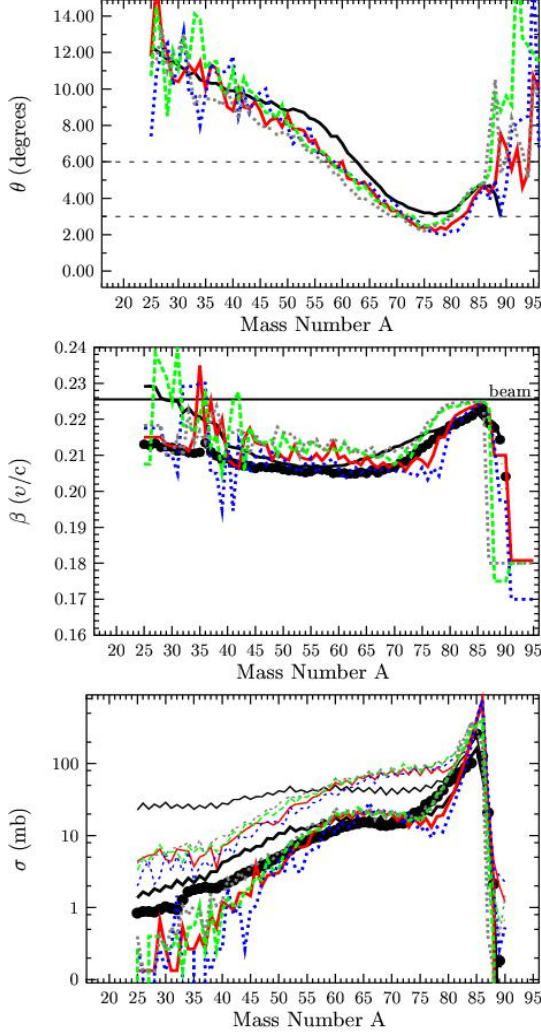


Figure 3. Mean angle (upper panel), mean velocity (middle panel) and yield (lower panel) as a function of projectile residue mass for the reaction ^{86}Kr (25MeV/nucleon) + ^{124}Sn . Black line: DIT. Blue (asy-soft), red (asy-stiff), green (super asy-stiff) and grey (no-symm): CoMD calculations (see text). Black points: MARS data [1]

In Fig. 5, upper panel, we show the calculated mean $(Z/A)^2$ of the primary quasiprojectiles as a function of the excitation energy per nucleon. The meaning of the curves is as in Fig. 2. The upper set of curves is for the $^{86}\text{Kr}(25\text{MeV/nucleon}) + ^{112}\text{Sn}$ reaction and the lower set is for the $^{86}\text{Kr}(25\text{MeV/nucleon}) + ^{124}\text{Sn}$ reaction. The solid horizontal line corresponds to the $(Z/A)^2$ of the projectile, whereas the upper and lower dashed lines give the $(Z/A)^2$ of the fully equilibrated systems in the two cases. In the lower panel of the figure we show the difference of the calculated mean $(Z/A)^2$ values, along

acceptance of the separator. Additionally, in the lower panel, the thin lines show the calculations of the total residue yields. We observe an overall satisfactory agreement of the CoMD calculations with the data and again, in the CoMD calculations, an insensitivity to the choice of the symmetry potential. The situation is similar for the

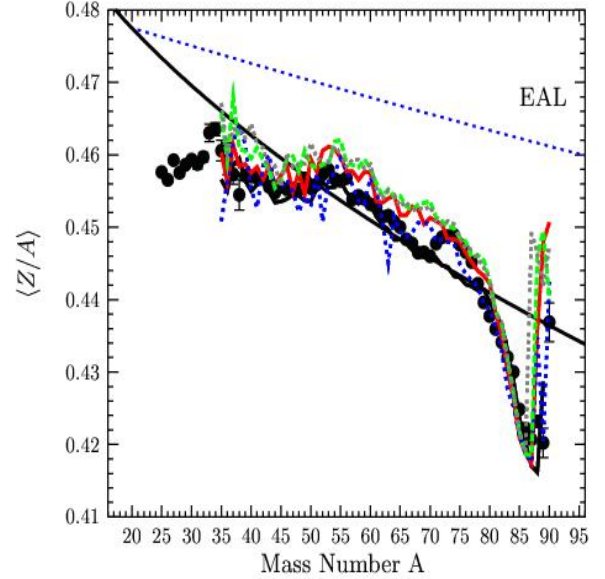


Figure 4. Mean projectile residue Z/A as a function of residue mass for the reaction $^{86}\text{Kr}(25\text{MeV/nucleon}) + ^{124}\text{Sn}$. Black line tracing the data: DIT. Blue (asy-soft), red (asy-stiff), green (super asy-stiff) and grey (no-symm): CoMD calculations (see text). Black points: MARS data [1]. Black line: line of stability.

comparison of the mean Z/A values of the observed residues with the CoMD calculations shown in Fig. 4.

with our data (solid and open points) from the heavy-residue isoscaling analysis of [4]. It is interesting to note that the CoMD calculations show sensitivity in the choice of the symmetry potential. However, this observation may be subject to the inherent uncertainty in the determination of the excitation energy of the quasiprojectiles. In the present calculations, the excitation energy has been determined from the difference of the binding energy of the (hot) quasiprojectiles as given by the CoMD code and the corresponding binding energy taken from mass tables. We have investigated the issues of the excitation energy determination and we believe that, except for very peripheral collisions (essentially corresponding to direct reactions) the CoMD code provides a reliable estimate of the excitation energies of the quasiprojectiles. The comparison presented in Fig. 5 suggests a rather stiff dependence of the symmetry energy on density (Fig. 1) in overall agreement with other studies, as presented in Ref. [7] (and references therein).

As part of our detailed consistency checks of the CoMD model framework, we report in Fig. 6 the predicted neutron skin of the ^{86}Kr nucleus using the four options of the symmetry potential. The values of the skin show a small sensitivity to the density dependence of the symmetry potentials and are in agreement with expectations from microscopic SHF or Thomas-Fermi calculations. In the same vein, Fig. 7 presents the giant dipole resonance (GDR) spectrum of the ^{86}Kr nucleus obtained from the Fourier transform of the spatial oscillation of the neutron vs proton spheres within the CoMD model. The symmetry potentials employed seem to give reasonable values for the GDR energy centroids (although somewhat lower than the value 16.8 MeV expected from empirical systematics [12,13]) and widths ~ 4 MeV in very good agreement with expectations for near ground-state nuclei [12].

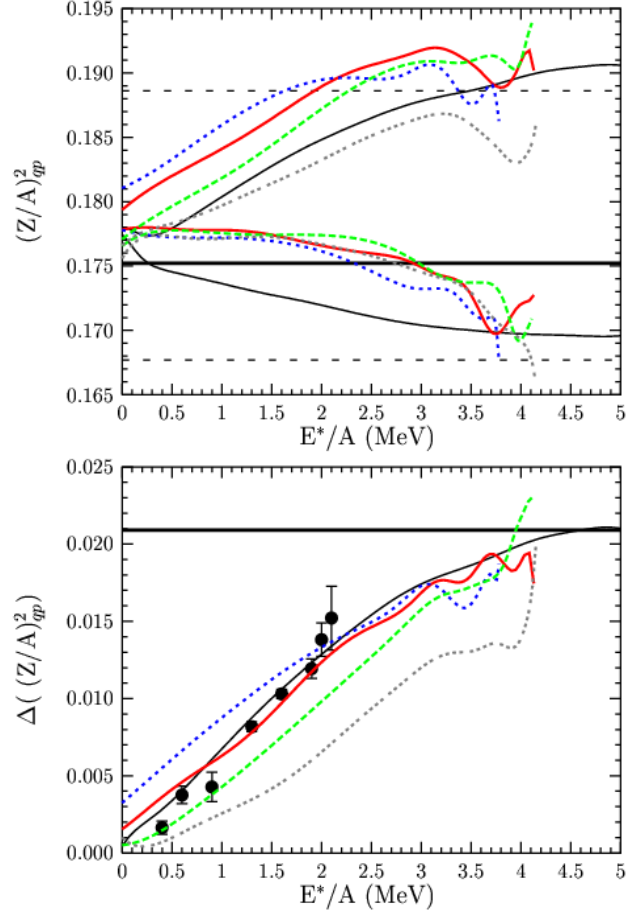


Figure 5. Upper panel: Mean $(Z/A)^2$ of quasiprojectiles as a function of excitation energy per nucleon for the 25 MeV/nucleon reactions: $^{86}\text{Kr} + ^{112}\text{Sn}$ (upper set of curves) and $^{86}\text{Kr} + ^{124}\text{Sn}$ (lower set of curves). Black lines DIT. Blue (asy-soft), red (asy-stiff), green (super asy-stiff) and grey (no-sym): CoMD calculations (see text). Lower panel: Difference in quasiprojectile mean $(Z/A)^2$. Lines as above.

Finally, we plan to explore the N/Z equilibration process (e.g., Fig. 5) in greater detail via comparisons of CoMD calculations with our new experimental data from 15 MeV/nucleon ^{40}Ar and ^{86}Kr projectiles on $^{64,58}\text{Ni}$ and $^{124,112}\text{Sn}$ targets that are currently under analysis.

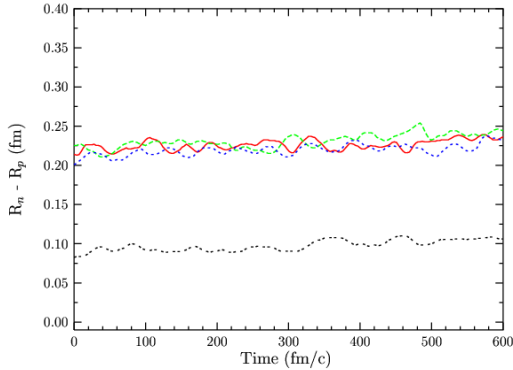


Figure 6. Time evolution of the neutron skin of an isolated ^{86}Kr nucleus predicted by CoMD. Blue (asy-soft), red (asy-stiff), green (super asy-stiff) and gray line (no-symm): choices of the nucleon symmetry potential (see text).

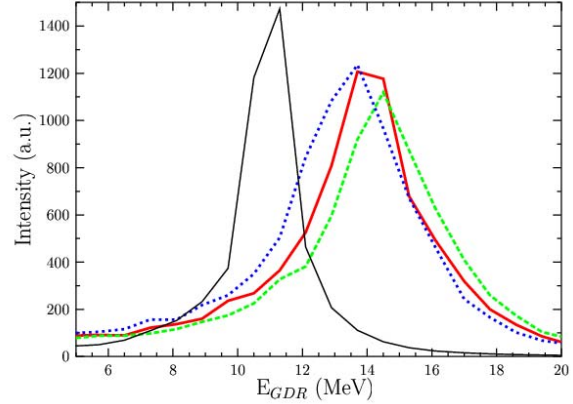


Figure 7. Giant dipole resonance (GDR) response of an isolated ^{86}Kr nucleus predicted by CoMD. Blue (asy-soft), red (asy-stiff), green (super asy-stiff) and black line (no-symm): choices of the nucleon symmetry potential (see text). The expected value of the energy according to the empirical GRD systematics is 16.8 MeV (see text) [12,13].

- [1] G. A. Souliotis *et al.*, Phys. Rev. Lett. **91**, 022701 (2003).
- [2] G. A. Souliotis *et al.*, Nucl. Instrum. Methods Phys. Res. **B204**, 166 (2003).
- [3] M. Veselsky and G. A. Souliotis, Nucl. Phys. **A765**, 252 (2006).
- [4] G. A. Souliotis *et al.*, Phys. Lett. B **588**, 35 (2004).
- [5] A. Ono and J. Randrup, Eur. Phys. J. A **30**, 109 (2006).
- [6] M. Papa *et al.*, Phys. Rev. C **64**, 024612 (2001).
- [7] M. Papa *et al.*, J. Comp. Phys. **208**, 403 (2005).
- [8] D. V. Shetty, S. J. Yennello, and G. A. Souliotis, Phys. Rev. C **76**, 024606 (2007).
- [9] L. Tassan-Got and C. Stephan, Nucl. Phys. **A524**, 121 (1991).
- [10] D. Lacroix *et al.*, Phys. Rev. C **69**, 054604 (2004).
- [11] R. Charity *et al.*, Nucl. Phys. **A483**, 391 (1988).
- [12] D. Santonocito and Y. Blumenfeld, Eur. Phys. J. A **30**, 183 (2006).
- [13] L. Trippa, G. Colo, and E. Vigezzi, [nucl-th] arXiv:0802.3658 (2008).